PLD-fabricated Pr-Fe-B thick film magnets applied to small motors

M. Nakano [iD], S. Takeichi, K. Inoue, K. Takashima, A. Yamashita, T. Yanai, and H. Fukunaga

COLLECTIONS

View Online   Export Citation   CrossMark

ARTICLES YOU MAY BE INTERESTED IN

PLD-fabricated Pr-Fe-B thick film magnets applied to small motors

View Online   Export Citation   CrossMark

M. Nakano,[a] [ID] S. Takeichi, K. Inoue, K. Takashima, A. Yamashita, T. Yanai, and H. Fukunaga

AFFILIATIONS

Graduate School of Engineering, Nagasaki University, Nagasaki 852-8521, Japan

Note: This paper was presented at the 64th Annual Conference on Magnetism and Magnetic Materials.
[a]**Corresponding author:** M. Nakano (mnakano@nagasaki-u.ac.jp).

ABSTRACT

Although a conventional isotropic Nd-Fe-B bonded magnet (coercivity: 800 kA/m, thickness: 350 μm) has been widely used for a miniaturized motor, deposition of a thick film magnet without resin directly on a small shaft enables us to advance the further reduction of the motor. When obtaining the film magnet on the shaft, we carried out fundamental experiments using a stainless plate. Namely, we investigated the mechanical characteristic such as adhesion together with magnetic properties of PLD (Pulsed Laser Deposition)-made films as a function of Pr content. It was found that Pr-Fe-B films with Pr content above 15 at. % tended to peel from the plates after the deposition. We suppose that the result is attributed to the different linear expansion coefficient between a stainless (10.3×10^{-6} K^{-1}) and Pr element (6.7×10^{-6} K^{-1}). On the other hand, an increase in Pr contents of the samples enabled us to enhance coercivity compared with that of a conventional Nd-Fe-B bonded magnet. In the study, we prepared a 250 μm-thick Pr-Fe-B film magnet with the coercivity (H_{cj}) of approximately 1250 kA/m on a thin stainless shaft applicable to a small motor by the PLD.

I. INTRODUCTION

Although Nd-Fe-B bonded magnets have been conventionally used for miniaturized motors,[1] the magnetic properties of the bonded ones are inferior to those of conventional sintered magnets because the bonded magnets contain a nonmagnetic phase such as thermosetting resin. Furthermore, reduction in the thickness of a magnet in the motors is required to obtain smaller motors. However, it is generally known that we have difficulty producing a bonded magnet thinner than 300 μm. Sputtering method was proposed to prepare thinner Nd-Fe-B magnets with good magnetic properties,[2–6] though it is difficult to obtain a sub millimeter thickness applied to a small motor due to a low deposition rate. On the other hand, although solidification of only Nd-Fe-B powder at high speed by using a plasma spray was effective to obtain a film magnet with a sub millimeter thickness,[7,8] magnetic polarization degraded because of the oxidation during the deposition. We, therefore, have prepared isotropic Nd-Fe-B film magnets with the thickness range from 10 to 1250 μm in vaccum atmosphere using a PLD method with high depsoition rate.[9] In addition, a 200 μm-thick PLD-made Nd-Fe-B

film was applied to an axial gap type DC brushless motor with a thickness of 0.8 mm and an outer diameter of 5 mm.[10] In the study, considering the demagnetization field due to the structure of a small motor aimed at development in this research, we need to increase the coercivity up to 1000 kA/m because permeance coefficient in a demagnetization curve is estimated at 1.0. Since the magnetic crystalline anisotropy constant of a $Pr_2Fe_{14}B$ phase ($K_u = 6.8$ MJ/m^3) is larger by approximately 2.3 MJ/m^3 than that of a $Nd_2Fe_{14}B$ phase ($K_u = 4.5$ MJ/m^3),[11] Pr-Fe-B thick film magnets instead of Nd-Fe-B ones were used.

This contribution reports the deposition of Pr-Fe-B films on stainless plates using a PLD method followed by same deposition process on stainless shafts to demonstrate a 250 μm-thick Pr-Fe-B film magnet with the coercivity above 1000 kA/m on a stainless shaft (diameter: approximately 0.5 mm) which is applicable to a small motor.

II. EXPERIMENTAL PROCEDURE

The detailed deposition conditions were shown in Table I. A Pr-Fe-B target was ablated with a Nd-YAG pulse laser (wavelength:

TABLE I. Conditions of deposition.

Target	$Pr_xFe_{14}B$ (x = 1.6~2.4)
Substrate (Plate, Shaft)	Stainless (SUS420J2)
Substrate-Target Distance	10 mm (Plate), 5 mm(Shaft)
Atmosphere (Before deposition)	$2.0~4.0\times10^{-5}$ Pa (Vacuum)
Deposition Time (Plate)	40 ~ 180 min
Deposition Time (Shaft)	14 h

355 nm) at the repetition rate of 30 Hz in vacuum atmosphere. The laser power, which was measured with a power meter in front of the entrance lens of a chamber, was approximately 4 W. Before the ablation, the chamber was evacuated down to approximately $2.0~4.0\times10^{-5}$ Pa by using a rotary pump together with a molecular turbo one. The distance between a target and a stainless plate was fixed at 10 mm. The area of all the obtained films on stainless plates was 5×5 mm^2. Average deposition rate exceeded approximately 40 μm/h. In the case of a stainless shaft, the distance between a target and a shaft with the diameter of approximately 0.5 mm was fixed at 5 mm. Average deposition rate was approximately 20 μm/h and the total deposition time was 14 h to obtain an approximately 300 μm-thick Pr-Fe-B film. The deposition was carried out using eight different positions to surround a film on a shaft. Namely, after depositing a Pr-Fe-B film for 1.75 h at a fixed position, the shaft was rotated by 45° followed by the deposition for 1.75 h. A Pr-Fe-B film could cover the whole shaft by repeating the deposition 8 times. A pulse annealing (PA)[12] was carried out to crystallize the films because all the as-deposited films had amorphous structure.

After the annealing process, samples were magnetized up to 7 T with a pulse magnetizer. As shown in Figs. 2 and 8, each film deposited on a plate and shaft had an isotropic magnetocrystalline anisotropy. J-H loops were measured with a VSM (Vibrating Sample Magnetometer) which could apply a magnetic field up to approximately 2000 kA/m reversibly. The in-plane magnetic field was applied for a stainless substrate. In the case of a stainless shaft, the magnetic field was applied in the longitudinal direction. The
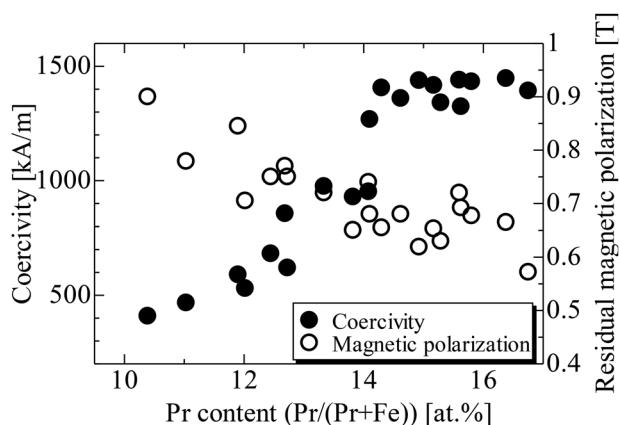

FIG. 2. X-ray diffraction patterns of as-deposited and annealed Pr-Fe-B films with each Pr content of 14.0 and 14.1 at. %, respectively, on stainless plates. The formation of $Pr_2Fe_{14}B$ crystalline phases through an annealing process could be confirmed.

composition of obtained films was evaluated with a SEM (Scanning Electron Microscope)-EDX (Energy Dispersive X-ray spectrometry), and the surface observation was also carried out by using a SEM. An average thickness was measured with a micrometer or estimated by measuring each weight.

III. RESULT AND DISCUSSION

Figure 1 shows the dependence of coercivity (H_{cj}) and residual magnetic polarization (J_r) on Pr content of films on stainless plates. As Pr contents increased, H_{cj} increased and J_r decreased. It is considered that the tendency is attributed to the increase in volume of non-magnetic phase at grain boundary and triple junction due to the increase in Pr contents. X-ray diffraction patterns of as-deposited and annealed Pr-Fe-B films with each Pr content of 14.0 and 14.1 at. %, respectively, on stainless plates were observed as shown in Fig. 2.

FIG. 1. Coercivity (H_{cj}) and residual magnetic polarization (J_r) of Pr-Fe-B films thicker than 10 μm deposited on stainless plates as a function of Pr content (Pr/(Pr+Fe)). Increase in Pr content increased H_{cj} and decreased J_r, respectively.
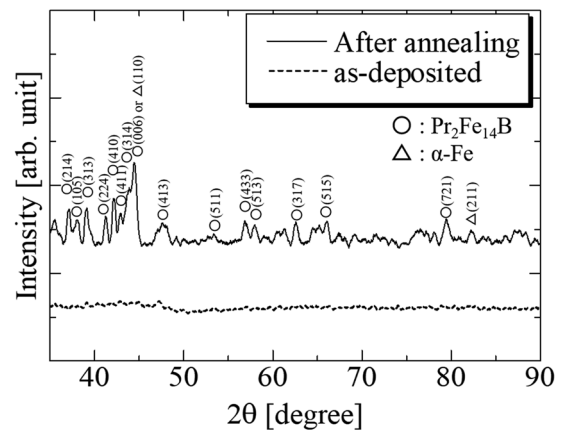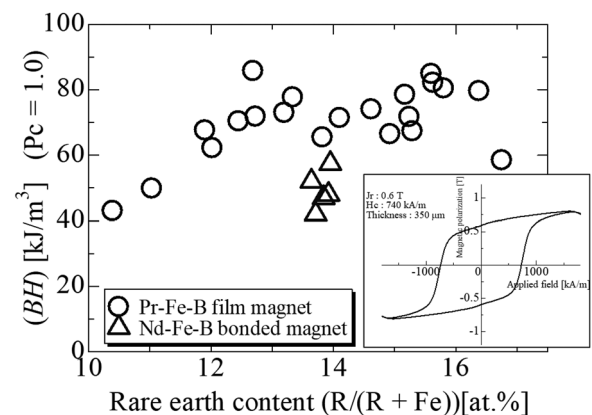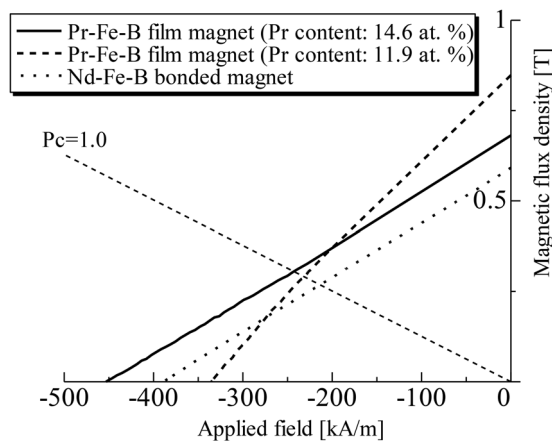

FIG. 3. Relationship between rare earth content and energy product ((BH)) at permeance coefficient of 1.0. (BH) values of Pr-Fe-B film magnets were larger than those of Nd-Fe-B bonded magnets. J-H loop of Nd-Fe-B one was also shown in the insert diagram.

FIG. 4. 2nd quadrant of *B-H* curves of two Pr-Fe-B film magnets with different Pr contents and a conventional Nd-Fe-B bonded magnet. (*BH*) values shown in Fig. 2 were calculated at the cross point between each curve and a line of permeance coefficient = 1.0.

TABLE II. Linear expansion coefficient of each material.

Material	Linear expansion coefficient ($\times 10^{-6}$ K^{-1})
Stainless steel (SUS420J2)	10.3
Fe	11.7
Pr	6.7

magnetic flux density (B_r) compared with those of the bonded magnet. In particular, high H_{cj} was effective to hold large magnetic flux density at $P_c = 1.0$. These results suggest that H_{cj} above 1000 kA/m is indispensable in a Pr-Fe-B film deposited on a shaft for a small motor.

In order to use the above-mentioned Pr-Fe-B films in a motor, mechanical characteristic was also examined. Figure 5 shows peeling phenomenon in as-deposited Pr-Fe-B films on stainless plates as

It was confirmed that the formation of $Pr_2Fe_{14}B$ crystalline phases enabled us to obtain hard magnetic properties of samples displayed in Fig. 1. Taking account of the demagnetization field due to the structure of a small motor aimed at development in the study, we estimated permeance coefficient in a demagnetization curve as 1.0. As seen in Fig. 3, evaluation on energy product ((BH)) at $P_c = 1.0$ as a function of rare earth (Pr or Nd) content in Pr-Fe-B film magnets on stainless plates and conventional Nd-Fe-B bonded magnets, respectively, was carried out. Here, a J-H loop of a conventional Nd-Fe-B one was also displayed as an inset. The (BH) values of Pr-Fe-B films were larger than those of Nd-Fe-B ones. In order to discuss the result of Fig. 3 in detail, the 2nd quadrant of B-H curves in three magnets were shown in Fig. 4. The two Pr-Fe-B films with different Pr contents show superior values of coercivity (H_{cb}) and/or residual
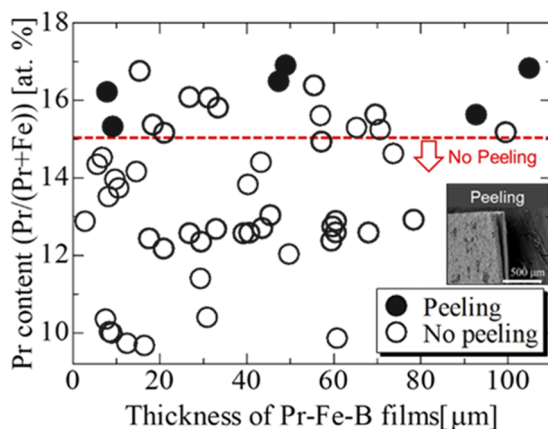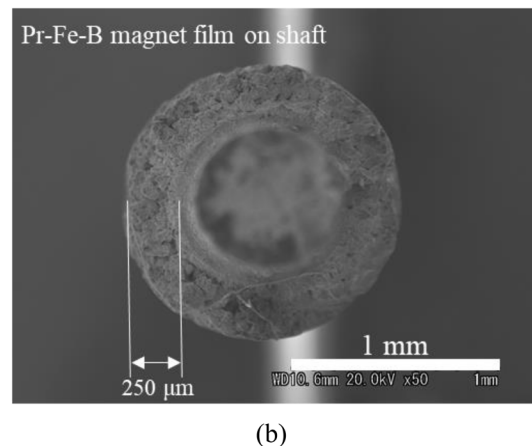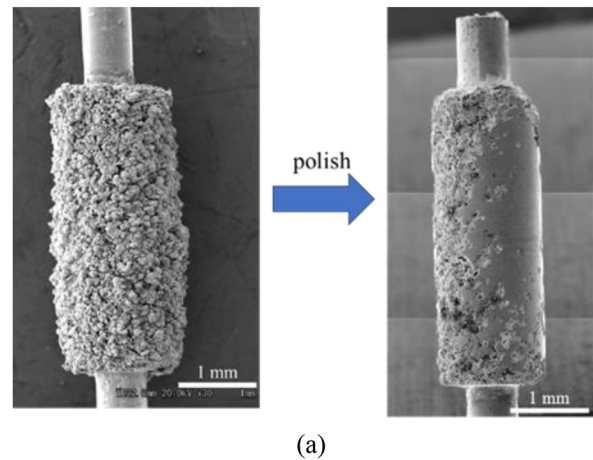

FIG. 5. Observation of peeling in as-deposited Pr-Fe-B films with various thicknesses and Pr content (Pr/(Pr+Fe)) on stainless plates. Peeling tended to occur in the Pr contents above 15. at %. Peeling phenomenon was also shown in the photo.


(a)

(b)

FIG. 6. Photos of Pr-Fe-B film magnets deposited on a thin stainless shaft. The surface of a film magnet was polished to obtain the uniform thickness of an approximately 250 μm. (a) Surface observation of as-deposited and polished films deposited on each shaft. (b) Cross sectional view of a polished film deposited on a shaft.
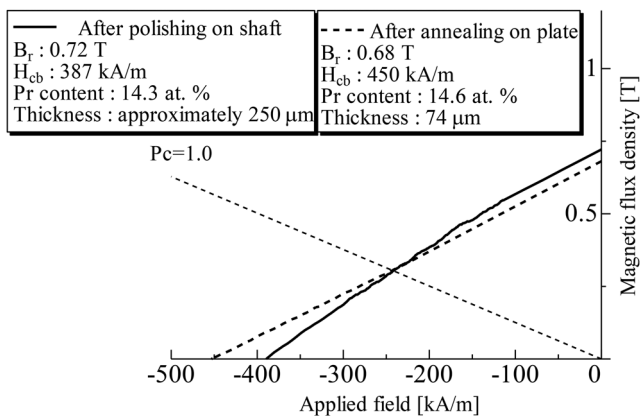
FIG. 7. 2nd quadrant of *B-H* curves of a Pr-Fe-B film magnet on a plate (see Fig. 4) together with a polished Pr-Fe-B film on a shaft, respectively. It was confirmed that the both (*BH*) values at permeance coefficient = 1.0 were almost the same.

Pr content and thickness varied. The films tended to peel from each plate when Pr contents exceeded 15 at. %. According to the previous experiment,[13] it is estimated that the temperature of a stainless plate raised up to at least 473 K during the deposition process. Since the linear expansion coefficient of a stainless (10.3×10^{-6} K^{-1}) is different from that of Pr element (6.7×10^{-6} K^{-1}) as shown in Table II, we suppose that the peeling phenomenon due to internal stress of the films occurred during the deposition process.

Since optimum Pr content range is considered to be from 14 to 15 at. %, a Pr-Fe-B thick film with the Pr content slightly below 15 at. % was deposited on a stainless shaft with the diameter of around 0.5 mm. Figure 6(a) shows photographs of an as-deposited Pr-Fe-B film together with an approximately 250 μm-thick Pr-Fe-B film magnet after polishing the surface. We didn't observe peeling phenomenon before and after the polishing process. In addition, we confirmed that the film could be surrounded on a shaft after the
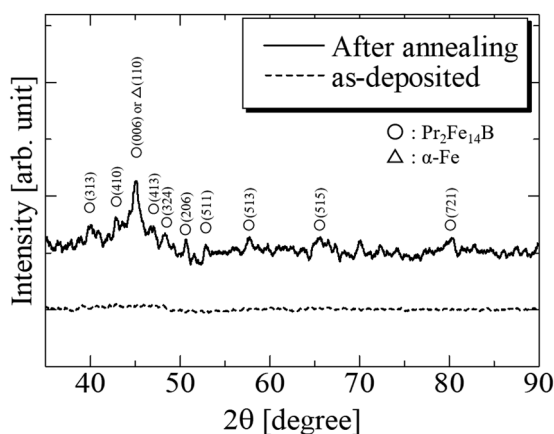
FIG. 8. X-ray diffraction pattern of an as-deposited Pr-Fe-B film with Pr content of 15.3 at. % on a stainless shaft. The as-deposited sample was annealed. The formation of $Pr_2Fe_{14}B$ crystalline phases through an annealing process could be confirmed.

polishing as displayed in Fig. 6(b). Figure 7 shows the comparison of a second quadrant of B-H loops of two samples. One is a Pr-Fe-B film magnet with Pr content of 14.6 at. % on a stainless plate shown in Fig. 4 and the other one is a polished Pr-Fe-B film with Pr content of 14.3 at. % on a stainless shaft. The values of energy product ((BH)) at P_c = 1.0 were 74 (plate) and 73 (shaft) kJ/cm^3, respectively. The evaluation on the energy product revealed that the magnetic properties of the two samples were comparable. An as-deposited Pr-Fe-B film with Pr content of approximately 15 at. % on a stainless shaft had amorphous structure as displayed in Fig. 8. Figure 8 also indicated that $Pr_2Fe_{14}B$ crystalline phases were formed by annealing the as-deposited sample. Namely, we confirmed that the formation of $Pr_2Fe_{14}B$ crystalline phases enabled us to obtain hard magnetic properties of a sample deposited on a shaft (see Fig. 7).

Consequently, it was clarified that a PLD-made Pr-Fe-B thick film magnet can contribute on the further reduction in a small motor.

IV. CONCLUSIONS

In order to develop a miniaturized motor, we clarified that a Pr-Fe-B thick film magnet deposited using a PLD method is a hopeful candidate instead a conventional bonded Nd-Fe-B magnet. It was found that the control of Pr content is indispensable to achieve not only high coercivity but also increase in thickness without mechanical destruction such as peeling. Resultantly, we could demonstrate a 250 μm-thick Pr-Fe-B film magnet on a stainless shaft with the diameter of approximately 0.5 mm.

REFERENCES

[1] S. Hirosawa and H. Tomizawa, J. Magn. Soc. Japan **21**, 160 (1997).
[2] N. M. Dempsey, A. Walther, F. May, D. Givord, K. Khlopkov, and O. Gutfleisch, Appl. Phys. Lett. **90**, 092509 (2007).
[3] Y. Zhang, D. Givord, and N. M. Dempsey, Acta Mater **60**, 3783 (2012).
[4] T. Kotouge, T. Fujita, Y. Tanaka, M. Uehara, K. Kanda, Y. Higuti, and I. Maenaka, Technical Meeting on Magnetics of IEE Japan, MAG-12-170, 7 (2012) (in Japanese).
[5] C. Zhi, T. Shinshi, and M. Uehara, Int. J. Autom. Technol. **7**, 196 (2013).
[6] R. Fujiwara, T. Shinshi, and E. Kazawa, Sens. Actuators A Phys. **220**, 298 (2014).
[7] G. Rieger, J. Wecker, W. Rodewald, W. Sattler, F.-W. Bach, T. Duda, and W. Unterberg, Journal of Applied Physics **87**, 5329 (2000).
[8] M. Willson, S. Bauser, S. Liu, and M. Huang, Journal of Applied Physics **93**, 7987 (2003).
[9] M. Nakano, H. Takeda, S. Sato, T. Yanai, F. Yamashita, and H. Fukunaga, Journal of Applied Physics **101**, 09K525 (2007).
[10] M. Nakano, R. Kato, S. Hoefinger, J. Fidler, F. Yamashita, and H. Fukunaga, Journal of Alloys and Compounds **408-412**, 1422 (2006).
[11] K. H. J. Buschow, *Handbook of Ferromagnetic Materials*, 4 (1988).
[12] H. Fukunaga, K. Tokunaga, and J. M. Song, IEEE Trans. Magn. **38**, 2970 (2002).
[13] M. Nakano, W. Oniki, T. Yanai, and H. Fukunaga, Journal of Applied Physics **109**, 07A723 (2011).